



**HAL**  
open science

## Study of human RIG-I polymorphisms identifies two variants with an opposite impact on the antiviral immune response.

Julien Pothlichet, Anne Burtey, Andriy V. Kubarenko, Grégory Caignard, Brigitte Solhonne, Frédéric Tangy, Meriem Ben-Ali, Lluís Quintana-Murci, Andrea Heinzmann, Jean-Daniel Chiche, et al.

### ► To cite this version:

Julien Pothlichet, Anne Burtey, Andriy V. Kubarenko, Grégory Caignard, Brigitte Solhonne, et al.. Study of human RIG-I polymorphisms identifies two variants with an opposite impact on the antiviral immune response.. PLoS ONE, 2009, 4 (10), pp.e7582. 10.1371/journal.pone.0007582. pasteur-00455204

**HAL Id: pasteur-00455204**

**<https://pasteur.hal.science/pasteur-00455204>**

Submitted on 11 Feb 2010

**HAL** is a multi-disciplinary open access archive for the deposit and dissemination of scientific research documents, whether they are published or not. The documents may come from teaching and research institutions in France or abroad, or from public or private research centers.

L'archive ouverte pluridisciplinaire **HAL**, est destinée au dépôt et à la diffusion de documents scientifiques de niveau recherche, publiés ou non, émanant des établissements d'enseignement et de recherche français ou étrangers, des laboratoires publics ou privés.

# Study of Human RIG-I Polymorphisms Identifies Two Variants with an Opposite Impact on the Antiviral Immune Response

Julien Pothlichet<sup>1,2</sup>, Anne Burtey<sup>1,2</sup>, Andriy V. Kubarenko<sup>3</sup>, Gregory Caignard<sup>4</sup>, Brigitte Solhonne<sup>1,2</sup>, Frédéric Tangy<sup>4</sup>, Meriem Ben-Ali<sup>5,6</sup>, Lluís Quintana-Murci<sup>5,6</sup>, Andrea Heinzmann<sup>7</sup>, Jean-Daniel Chiche<sup>8</sup>, Pierre-Olivier Vidalain<sup>4</sup>, Alexander N. R. Weber<sup>3</sup>, Michel Chignard<sup>1,2</sup>, Mustapha Si-Tahar<sup>1,2,8\*</sup>

**1** Institut Pasteur, Unité de Défense Innée et Inflammation, Paris, France, **2** Inserm, U874, Paris, France, **3** Deutsches Krebsforschungszentrum, Toll-Like Receptors and Cancer, Heidelberg, Germany, **4** Institut Pasteur, Laboratoire de Génétique Virale et Vaccination, Paris, France, **5** Institut Pasteur, Unité postulante de Génétique Evolutive Humaine, Paris, France, **6** CNRS, URA3012, Paris, France, **7** Centre for Pediatrics and Adolescent Medicine, University of Freiburg, Freiburg, Germany, **8** Assistance Publique-Hôpitaux de Paris, Hôpital Cochin, Unité de Réanimation Médicale, Paris, France

## Abstract

**Background:** RIG-I is a pivotal receptor that detects numerous RNA and DNA viruses. Thus, its defectiveness may strongly impair the host antiviral immunity. Remarkably, very little information is available on RIG-I single-nucleotide polymorphisms (SNPs) presenting a functional impact on the host response.

**Methodology/Principal Findings:** Here, we studied all non-synonymous SNPs of RIG-I using biochemical and structural modeling approaches. We identified two important variants: (i) a frameshift mutation (P<sub>229</sub>fs) that generates a truncated, constitutively active receptor and (ii) a serine to isoleucine mutation (S<sub>183</sub>I), which drastically inhibits antiviral signaling and exerts a down-regulatory effect, due to unintended stable complexes of RIG-I with itself and with MAVS, a key downstream adapter protein.

**Conclusions/Significance:** Hence, this study characterized P<sub>229</sub>fs and S<sub>183</sub>I SNPs as major functional RIG-I variants and potential genetic determinants of viral susceptibility. This work also demonstrated that serine 183 is a residue that critically regulates RIG-I-induced antiviral signaling.

**Citation:** Pothlichet J, Burtey A, Kubarenko AV, Caignard G, Solhonne B, et al. (2009) Study of Human RIG-I Polymorphisms Identifies Two Variants with an Opposite Impact on the Antiviral Immune Response. PLoS ONE 4(10): e7582. doi:10.1371/journal.pone.0007582

**Editor:** David M. Ojcius, University of California Merced, United States of America

**Received:** August 4, 2009; **Accepted:** October 1, 2009; **Published:** October 27, 2009

**Copyright:** © 2009 Pothlichet et al. This is an open-access article distributed under the terms of the Creative Commons Attribution License, which permits unrestricted use, distribution, and reproduction in any medium, provided the original author and source are credited.

**Funding:** This study was partially funded by the Institut Pasteur through three "Programme Transversal de Recherche" (PTR#186, PTR#1224 and PTR#202) and by the French national research agency (ANR-MIE-Flupropar and ANR-MIE-Evolvsensors). Alexander N. R. Weber and Andriy V. Kubarenko are funded by Deutsche Forschungsgemeinschaft and Deutsches Krebsforschungszentrum. Gregory Caignard is supported by a "Bourse de Docteur Ingenieur" from Centre National de la Recherche Scientifique (CNRS). The funders had no role in study design, data collection and analysis, decision to publish, or preparation of the manuscript.

**Competing Interests:** The authors have declared that no competing interests exist.

\* E-mail: sitahar@pasteur.fr

## Introduction

Among all viral components that trigger the antiviral screen of the host, nucleic acids have been viewed as the most important [1]. In mammals, there are at least two receptor systems in place to detect such viral motifs and to further mount a type I interferon (IFN)-dependent antiviral immune response. The endosomal TLR3, 7, 8, and 9 interact with extracellular viral nucleic acids while the cytosolic helicases RIG-I and MDA-5 sense intracellular double-stranded (ds)RNA and/or 5' triphosphate single-stranded RNA, two common byproducts of viral infection and replication [2,3,4,5].

Current knowledge posits RIG-I as a particularly critical surveillance molecule that detects numerous viruses such as the human pathogens influenza and hepatitis C (HCV) viruses [6,7]. RIG-I interacts with its ligands by means of its central ATP-binding helicase domain as well as its carboxyterminal regulatory domain (RD; see the schematic representation in Fig. 1A). *Via* its amino-terminal tandem Caspase Recruitment Domains (CARDs), RIG-I

homocomplexes relay a signal by binding MAVS (also known as IPS-1, CARDIF or VISA), an adapter protein that mediates CARD-dependent interactions with RIG-I. This signaling complex further activates the transcription factors NF- $\kappa$ B and interferon regulatory factor (IRF)-3 to ultimately upregulate the expression of pro-inflammatory and antiviral mediators and the subsequent induction of adaptive immune responses [2,3,4].

Importantly, the receptor function of RIG-I is non-redundant, as confirmed by knock-out studies [8]. Moreover, the Huh7.5 hepatocytic cell line is especially permissive to HCV as the result of an elaborate viral evasion strategy as well as to a defective RIG-I protein bearing a single mutation [9,10]. In that regard, unequivocal evidence shows that genetic mutations may be important determinants of increased susceptibility to viral diseases [11,12]. Among them, single-nucleotide polymorphisms (SNPs) are DNA sequence variations that occur when a single nucleotide is altered. There are more than 4 million SNPs in the human genome, 200,000 of which occur in coding regions, underlying the extent of genetic variability

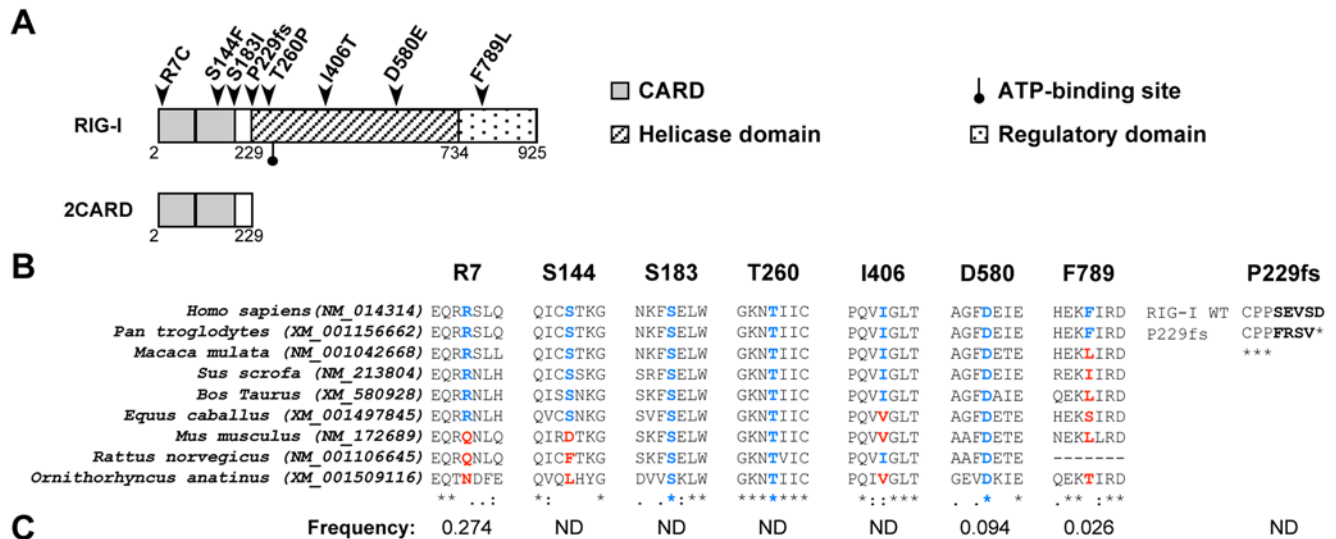


**Figure 1. Genetic variability profile of human RIG-I.** (A) Schematic representation of major domains of RIG-I (adapted from [7,17,34]). RIG-I non-synonymous SNPs described in NCBI SNP database are indicated as R<sub>7</sub>C (rs10813831), S<sub>144</sub>F (rs55789327), S<sub>183</sub>I (rs11795404), P<sub>229</sub>frameshift (fs) (rs36055726), T<sub>260</sub>P (rs35527044), I<sub>406</sub>T (rs951618), D<sub>580</sub>E (rs17217280), F<sub>789</sub>L (rs35253851). (B) Alignment of protein sequence of RIG-I SNPs from human to platypus, using ClustalW software. Amino acids in blue and red correspond to conserved and non-conserved residues, respectively. (C) Frequency of RIG-I SNPs alleles. This latter information was collected from NCBI SNP database and refers to the sum of SNP containing alleles in both homozygous and heterozygous individuals for a given SNP. ND: not determined. doi:10.1371/journal.pone.0007582.g001

and its potential positive or negative effects on the host antimicrobial defense [13,14]. Interestingly, studies aiming to characterize RIG-I polymorphisms are scarce. Here, we characterized functional effects of two RIG-I SNPs that might help us to understand the basis of individual variations between normal and abnormal innate immune responses to viral pathogens as well as to better appreciate the molecular mechanism by which RIG-I is triggered by non-self RNA.

## Results

### Genetic variability profile of human RIG-I

Information collected on 04/2009 from NCBI SNP database indicates that at least 342 SNPs are present in the human RIG-I gene. Among them, 14 are situated within coding sequences but only 7 result in amino acids substitutions, *i.e.* R<sub>7</sub>C, S<sub>144</sub>F, S<sub>183</sub>I, T<sub>260</sub>P, I<sub>406</sub>T, D<sub>580</sub>E, F<sub>789</sub>L (Fig. 1A). An additional SNP corresponds to a thymidine insertion at nucleotide position 845 of RIG-I mRNA (accession number NM\_014314), which results in a frameshift (fs) and in a truncated RIG-I protein. This mutant is herein defined as P<sub>229</sub>fs as it includes the first 229 residues (instead of 925 residues in the WT RIG-I protein) followed by 4 unintended residues (*i.e.* FRSV; Fig. 1B) and thus, does not contain the helicase and the RD domains. As illustrated in Fig. 1A, RIG-I SNPs map to the different domains of the protein.

Next, we found by sequence alignments, that the S<sub>183</sub>I, T<sub>260</sub>P, I<sub>406</sub>T and D<sub>580</sub>E mutations affect amino acids that are rather conserved in all analyzed species, whereas R<sub>7</sub>C, S<sub>144</sub>F and F<sub>789</sub>L affect residues conserved only in higher mammals (Fig. 1B). In regard to RIG-I SNP frequency in a healthy randomly selected human population, the NCBI SNP database provides such information for only three SNPs among the eight described here (R<sub>7</sub>C, D<sub>580</sub>E and F<sub>789</sub>L; Fig. 1C). The frequency values provided are very low and may suggest a negative selection of these SNPs due to their impact on RIG-I function. To check this hypothesis, we further studied the functional impact of all missense SNPs on RIG-I function.

### Missense SNPs differentially affect RIG-I-mediated innate immune signaling

Elucidating the functional role of non-synonymous SNPs in RIG-I may enhance our understanding of viral pathogenesis and host defense mechanisms as well as to contribute to a more detailed knowledge in structure-function relationship of RIG-I. To this effect, plasmids containing the eight SNPs were generated by site-directed PCR mutagenesis. We first observed that R<sub>7</sub>C, S<sub>144</sub>F, S<sub>183</sub>I, P<sub>229</sub>fs, T<sub>260</sub>P, I<sub>406</sub>T, D<sub>580</sub>E, F<sub>789</sub>L mutations did not alter expression and/or stability of RIG-I protein using western-blot (Fig. 2A) and flow cytometry (Fig. 2B) analyses. Also, the molecular weight of all RIG-I proteins was similar, with the exception of P<sub>229</sub>fs RIG-I which resulted in a truncated protein with a size comparable to the 2CARD module (Fig. 2A).

To determine whether non-synonymous SNPs can alter RIG-I-induced antiviral and/or pro-inflammatory signaling pathways, we used a functional cell-based assay to evaluate RIG-I-dependent activation of an IFN- $\beta$  promoter or an NF- $\kappa$ B- or IRF-3-dependent promoter, respectively. We first checked the level of constitutive activation of the RIG-I constructs in absence of any stimulus in HEK 293T or BEAS-2B cells. Fig. 2C shows a moderate but highly significant constitutive IFN- $\beta$  expression and IRF-3 activity -but no NF- $\kappa$ B activity (not shown)- in WT RIG-I-transfected cells ( $n = 3$ ,  $p < 0.001$  when compared to control vector-expressing cells), in agreement with the fact that RIG-I is especially prominent in signaling pathways leading to type I IFNs [2,3,4,15]. Interestingly, IFN- $\beta$  expression and IRF-3 activity in cells expressing T<sub>260</sub>P, I<sub>406</sub>T or F<sub>789</sub>L mutants was similar to that induced by WT RIG-I and lower in cells expressing the R<sub>7</sub>C, S<sub>144</sub>F, or D<sub>580</sub>E RIG-I ( $n = 3$ ,  $p \leq 0.0002$ ). With regard to P<sub>229</sub>fs RIG-I, we observed a salient constitutive IFN- $\beta$  and NF- $\kappa$ B reporter activities, at a level well above that induced by the full-length form of WT RIG-I ( $n = 3$ ,  $p < 0.0001$ ; Fig. 2D). In addition, P<sub>229</sub>fs SNP induces the expression of endogenous inflammatory and antiviral chemokines such as IL-8 and RANTES, respectively (Fig. 2E), at a level comparable to that

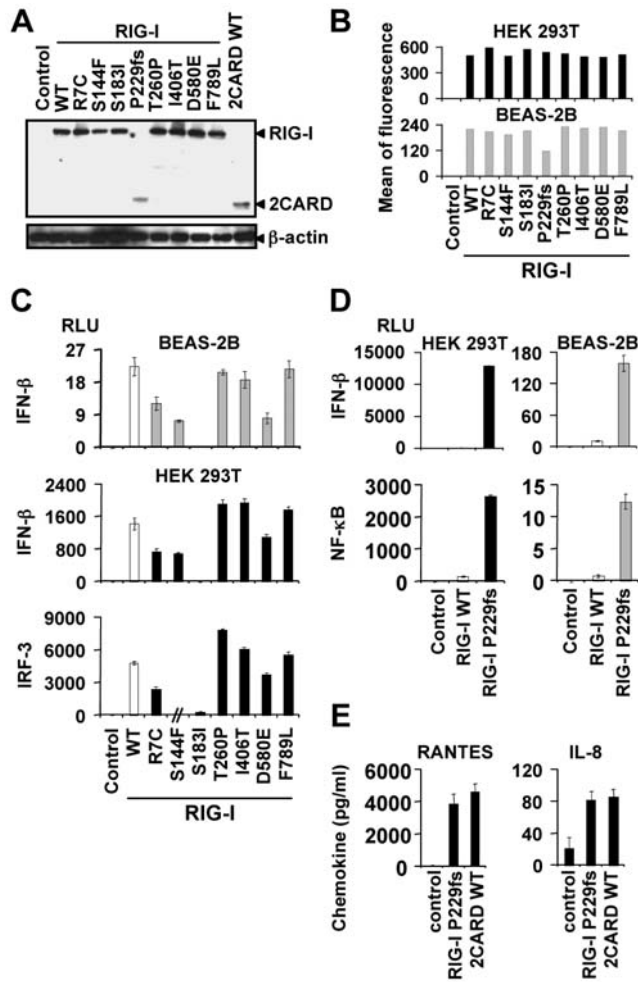


**Figure 2. RIG-I-mediated constitutive innate immune signaling, but not expression level, is differentially affected by RIG-I SNPs.** Expression of wild-type (WT) and non-synonymous SNPs RIG-I as assessed by western-blot using BEAS-2B cells (A) and flow cytometry (B) using an anti-Flag antibody and BEAS-2B and/or HEK 293T cells 42 h post-transfection. RIG-I SNP proteins are expressed at the same level as WT RIG-I with the exception of P<sub>229fs</sub> in BEAS-2B cells. (C–E) BEAS-2B (grey bars) and/or HEK 293T cells (black bars) were co-transfected with a  $\beta$ -galactosidase reporter plasmid and either a NF- $\kappa$ B-, IRF-3 or IFN- $\beta$ -luciferase-reporter plasmid and a vector encoding WT (empty bars) or SNPs RIG-I (filled bars) (C–E) or WT 2CARD (E) or a control plasmid. Data were collected 42 h (C) or 24 h (D–E) post-transfection and are expressed as the mean  $\pm$  SD of RLU normalized to  $\beta$ -galactosidase activity of triplicate samples minus basal activity measured in empty vector-transfected cells (C–D). One representative experiment out of three is shown. // in (C) means that this condition was not tested. (E) Stimulated HEK 293T cells as shown in panels (D) were assessed for IL-8 and RANTES release by ELISA. Data are mean  $\pm$  SD of triplicate samples and are representative of three independent experiments. doi:10.1371/journal.pone.0007582.g002

triggered by the 2CARD module. This finding is particularly important as it suggests that individuals carrying such mutation may constitutively produce exaggerated amounts of immune mediators.

By contrast, no constitutive IFN- $\beta$  expression was triggered by the S<sub>183I</sub> RIG-I mutant ( $n = 3$ ,  $p < 0.0001$ ; Fig. 2C). More importantly, S<sub>183I</sub> SNP uniquely inhibited IRF-3 (not shown), IFN- $\beta$  and NF- $\kappa$ B reporter activities elicited by the viral mimetic poly(I:C), in agreement with previous studies that have shown that poly(I:C) is a potent RIG-I stimulus ([16,17,18,19]; Fig. 3A;  $n = 3$

$p < 0.0001$ ). To confirm the pathophysiological relevance of the above findings, we sought to address the responsiveness of the mutant proteins to viral infection. We clearly demonstrated that S<sub>183I</sub> mutation had a deleterious effect on RIG-I antiviral activity as it drastically reduced IFN- $\beta$  and NF- $\kappa$ B-mediated responses triggered by intact, replicative Sendai or influenza A viruses (Fig. 3B and 3C). Noteworthy, while R<sub>7C</sub> SNP slightly inhibited RIG-I signaling triggered by Sendai virus stimulation, D<sub>580E</sub> inhibited RIG-I signaling in response to dsRNA and IAV, but not to Sendai virus infection ( $n = 3$ ,  $p \leq 0.003$ ). Nevertheless, as S<sub>183I</sub> SNP uniquely resulted in the strongest inhibition of RIG-I-dependent signaling induced by all stimuli, we decided to focus the rest of our study on this specific mutation. Thus, the clear loss-of-function effect of S<sub>183I</sub> RIG-I was confirmed by measuring the secretion of IL-8 ( $n = 3$ ,  $p < 0.0001$ ; Fig. 3D) and RANTES (not illustrated) in the supernatants of stimulated HEK 293T cells. This result well extends Shigemoto *et al.*'s findings using RIG-I-deficient murine embryonic fibroblasts [20]. Finally, specificity controls are

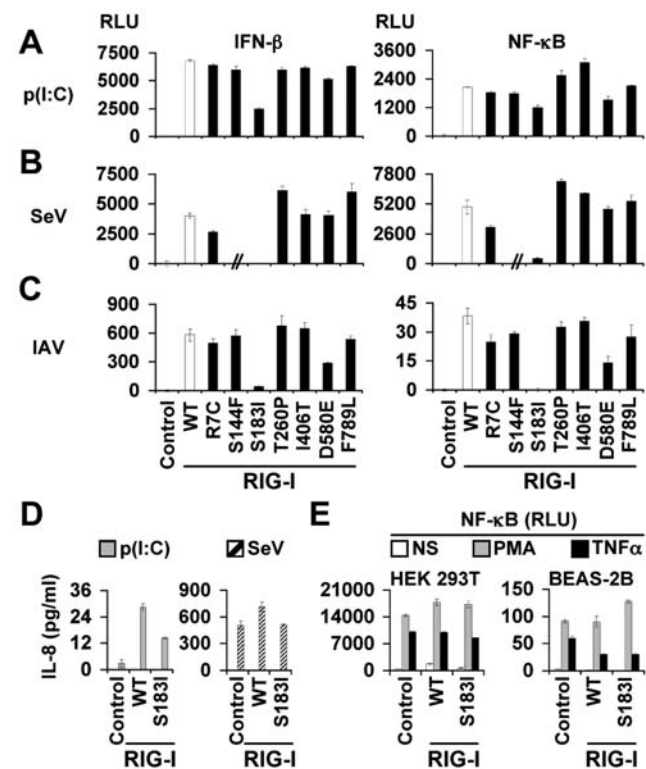


**Figure 3. SNPs differentially modulate RIG-I-mediated immune signaling in response to a viral dsRNA mimetic as well as to influenza A and Sendai viruses.** HEK 293T cells (A–B) and BEAS-2B cells (C) were co-transfected with WT (open bars) or non-synonymous SNP RIG-I (black bars) expression vectors and IFN- $\beta$  or NF- $\kappa$ B-dependent luciferase reporter plasmids. 24 h later, cells were challenged for 18 h by poly(I:C) (A) or infected with Sendai virus (SeV, 2 HAU/well) (B) or influenza A virus (IAV, MOI = 1) (C). Data are expressed as in Fig. 2c and are representative of three independent experiments. // in (B) means that this condition was not tested. (D) The stimulated or infected cells as shown in panels (A–B) were subsequently assessed for IL-8 release by ELISA. Data are mean  $\pm$  SD of triplicate samples and are representative of three independent experiments. IL-8 was undetectable in supernatants of non-stimulated transfected cells. (E) S<sub>183I</sub> SNP does not alter RIG-I-independent signaling. BEAS-2B and HEK 293T cells were co-transfected with WT or S<sub>183I</sub> RIG-I vectors or empty vector (control) and a NF- $\kappa$ B-dependent luciferase reporter plasmid. 24 h later cells were stimulated with PMA (100 nM) or TNF- $\alpha$  (20 ng/ml). doi:10.1371/journal.pone.0007582.g003

provided to make sure the alteration of cell signaling by S183I variant is specific to the RIG-I-dependent pathway. Thus, NF- $\kappa$ B signaling in HEK 293T or BEAS2B cells triggered by two non-viral stimuli (*i.e.* the cytokine TNF $\alpha$  and the potent PKC signaling activator PMA) was not down-modulated by S<sub>183</sub>I RIG-I, in comparison with WT RIG-I (Fig. 3E). Altogether, these data stressed the critical role of S<sub>183</sub> residue in mediating RIG-I-induced innate immune signaling.

### RIG-I 2CARD module carrying the S<sub>183</sub>I SNP is unable to trigger signal transduction

Next, we investigated the mechanism by which S<sub>183</sub>I SNP results in inhibition of RIG-I antiviral immune response. First, we found that this was neither due to an alteration at a very early step of RIG-I signaling, *i.e.* the ligand-binding capacity (Fig. 4A) nor to a RIG-I cellular mislocalization (not illustrated). In a very recent report, Fujita's laboratory also demonstrated that the inhibitory phenotype of S<sub>183</sub>I RIG-I was neither due to a failure of ubiquitination [20]; a post-translational process essential for RIG-I activity [21]. Next, we took advantage of the fact that the isolated tandem WT 2CARD elicits a vigorous and spontaneous induction of downstream signaling [7] to examine whether S<sub>183</sub>I mutation could also inhibit this constitutive cell response. As shown in Fig. 4B, contrary to WT 2CARD, the S<sub>183</sub>I 2CARD could not induce IFN- $\beta$  and NF- $\kappa$ B activities in HEK 293T ( $n = 3$ ,  $p < 0.0001$ ) and BEAS-2B cells (not shown). This loss-of-function effect was confirmed by measuring the secretion of endogenous mediators in supernatants of HEK 293T cells ( $n = 3$ ,  $p < 0.0001$ ; Fig. 4C).

### RIG-I isoleucine 183 residue closes off RIG-I homodimers and RIG-I/MAVS complexes

CARD domains mediate homotypic or heterotypic interactions

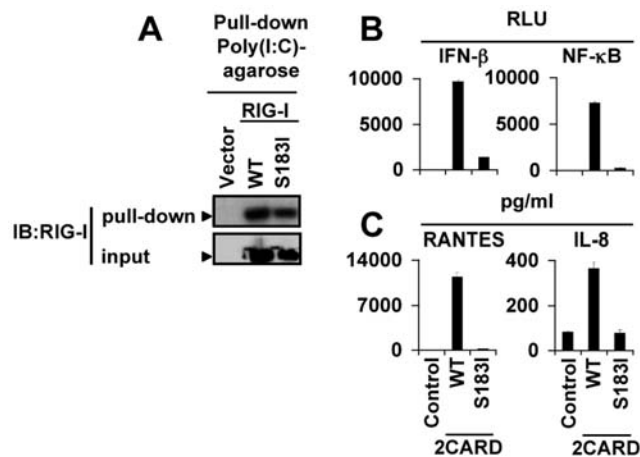


**Figure 4. Analysis of the loss-of-function mechanism of S<sub>183</sub>I SNP: evidence for an inhibition of the constitutive signal transduction triggered by 2CARD RIG-I.** (A) S<sub>183</sub>I does not affect dsRNA binding activity of RIG-I as assessed by a pull-down of Flag-tagged WT and S<sub>183</sub>I RIG-I proteins using poly(I:C)-coated agarose beads, 42 h after transfection of HEK 293T cells. (B, C) S<sub>183</sub>I strongly inhibits RIG-I 2CARD-induced IFN- $\beta$ -dependent antiviral and NF- $\kappa$ B-dependent pro-inflammatory signaling as demonstrated by luciferase reporter assays (B) or by measuring RANTES and IL-8 release by ELISA in HEK 293T cells (C) co-transfected for 42 h with WT or S<sub>183</sub>I 2CARD or empty expression vector and luciferase reporter plasmids. Data are mean  $\pm$  SD of triplicate samples and are representative of three independent experiments.

doi:10.1371/journal.pone.0007582.g004

to promote signaling events [22,23]. It is therefore possible that S<sub>183</sub>I SNP inhibits downstream signaling by altering RIG-I oligomerization or RIG-I/MAVS interaction. To test this hypothesis, we first examined the formation of RIG-I complexes between WT or S<sub>183</sub>I RIG-I and the constitutively active WT 2CARD. A detailed kinetic analysis revealed that this oligomerization process was dynamic with WT RIG-I complexes detectable as early as 16 h and a peak of interaction at 30 h post-transfection followed by a dissociation 40 h post-transfection ( $n = 6$ ; Fig. 5A). Remarkably, we observed that S<sub>183</sub>I RIG-I formed a more prominent complex with WT 2CARD at any time point, suggesting that this SNP increases RIG-I self-association.

Previous studies have demonstrated that RIG-I engages MAVS through CARD-mediated interactions, leading to the activation of downstream transcriptional factors essential for effective antiviral responses [2,3,4]. Thus, we further assessed whether S<sub>183</sub>I SNP could also influence RIG-I/MAVS complex formation. Using a co-immunoprecipitation approach, a kinetic analysis first revealed that WT 2CARD/MAVS interaction was also dynamic with complexes detectable in cells transfected with vectors encoding WT proteins, as early as 18 h and increasing at 30 h post-transfection ( $n = 3$ ; Fig. 5B). Remarkably, we observed that S<sub>183</sub>I SNP also enhanced 2CARD/MAVS complexes (Fig. 5B) as well as full-length RIG-I/MAVS interaction induced by Sendai virus (Fig. 5C). Collectively, our data reveal the importance of S<sub>183</sub> in the transient complex formation that is required for proper RIG-I-mediated signaling pathways and strongly support the hypothesis that regulation of RIG-I/RIG-I and RIG-I/MAVS association/dissociation constitutes a major checkpoint of this antiviral signaling.

As S<sub>183</sub>I is located in the RIG-I second CARD (CARD#2) domain, we next postulated that this paradoxical enhancing effect of S<sub>183</sub>I SNP might be due to CARD structure alteration. Using sequence alignment information (*cf.* Fig. S1) and a previously described homology modeling approach [24], we generated three-dimensional homology models for the RIG-I CARD#2 structure as well as its S<sub>183</sub>I variant. As shown in Fig. 5D, residue 183 is located on the helix 6 of CARD#2. Interestingly, when subjected to a 10 ns molecular dynamics simulation (last frame shown in Fig. 5D; intermediate frames illustrating behavior during simulation are available in Fig. S2), WT and mutant structures behaved differently as to the position of helix 6. Whereas in the WT protein helix 6 is at an approximately 60° angle to the remaining helices, in the S<sub>183</sub>I variant, helix 6 is tightly packed in an almost parallel way, leading to differences in surface structure and hydrophobicity (Figs. 5E,F). For instance, WT CARD#2 shows a hydrophobic patch involving I<sub>187</sub> and V<sub>188</sub> in the vicinity of S<sub>183</sub>, whereas this patch is absent in the mutant structure and a new hydrophobic patch surrounds I<sub>132</sub>. While the overall charge distribution appears unchanged, the relative spatial arrangement of charged residues is altered by the S<sub>183</sub>I substitution (Fig. 5F, see *e.g.* the negatively charged E<sub>176</sub>, E<sub>184</sub> or the positively charged K<sub>169</sub>, K<sub>172</sub>, K<sub>177</sub> and K<sub>181</sub>). Additionally, comparison of the movement of secondary structure elements over the course of the simulation suggests the S<sub>183</sub>I structure is less flexible than the WT structure (Fig. S3).

### S<sub>183</sub>I SNP exerts a down-modulatory effect

Phenotypes of several heritable disorders are linked to missense mutations in single alleles. In some cases, the mutant protein exhibits a regulatory effect whereby heterozygous co-expression of mutant and WT gene has a deleterious consequence, relatively to the case in which two WT alleles are expressed [25,26]. Such a down-regulatory effect usually involves homomeric or heteromeric proteins. In regard to the ability of S<sub>183</sub>I SNP to impair antiviral

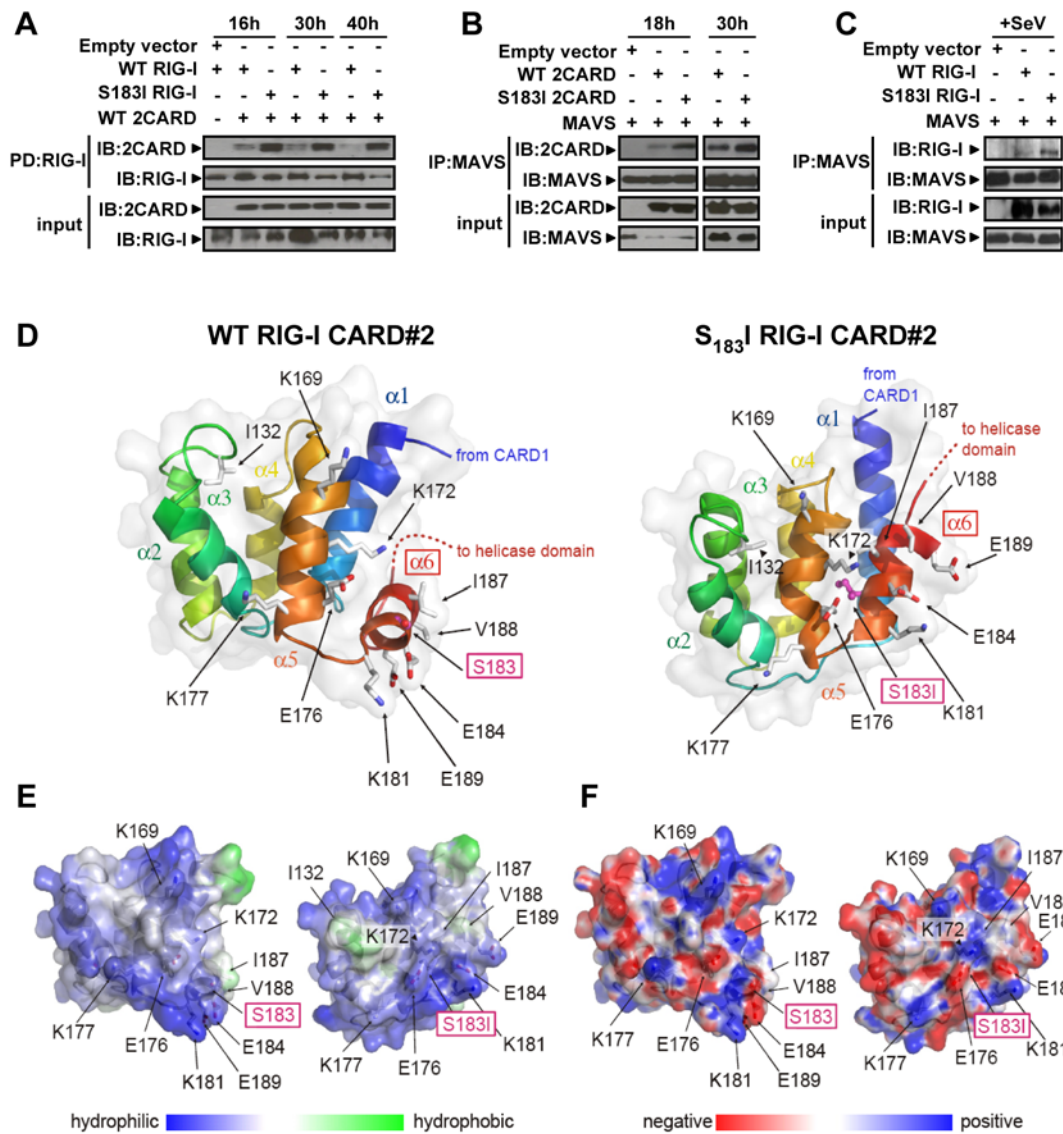


**Figure 5. S<sub>183</sub>I RIG-I SNP increases RIG-I/RIG-I and RIG-I/MAVS interactions.** (A) Kinetic of 2CARD/RIG-I interaction was analyzed in HEK 293T cells co-transfected with biotin-WT RIG-I or biotin-S<sub>183</sub>I RIG-I and Flag-WT 2CARD expression vectors. Biotin-RIG-I proteins were pull-downed and revealed as described in Methods section. (B) Kinetic of 2CARD/MAVS interaction was assessed in HEK 293T cells co-transfected with V5-WT or S<sub>183</sub>I 2CARD and Flag-MAVS. MAVS was immunoprecipitated with an anti-Flag antibody and interaction with 2CARD was revealed by immunoblot with an anti-V5 antibody. (C) Full-length RIG-I/MAVS interaction was evaluated in HEK 293T cells co-transfected with biotin-WT or -S<sub>183</sub>I RIG-I and Flag-MAVS expression vectors for 25 h and infected with Sendai virus for 19 h. MAVS was immunoprecipitated as in (B) and complexes with RIG-I were detected with streptavidin-HRP. IP: immunoprecipitation; PD: pull-down; IB: immunoblot. (D–F) Structural modeling suggests differences between WT and S<sub>183</sub>I second CARD (CARD#2) domain of RIG-I. (D) a three-dimensional homology model of the CARD#2 (residues 92–193) of WT (left) and S<sub>183</sub>I (right) RIG-I was subjected to a 10 ns molecular dynamics simulation. The last frame is shown. Helices are numbered and color coded and amino acid 183 shown in pink and boxed. As evident, helix  $\alpha$  (6), which harbors amino acid I<sub>183</sub>, shows a different spatial orientation. (E) Surface hydrophobicity is affected by this structural rearrangement, in particular a small patch surrounding I<sub>187</sub> and V<sub>188</sub> in WT (left), and I<sub>132</sub> in S<sub>183</sub>I (right) CARD#2, respectively. Hydrophobicity near the N-terminus of H1 is due to truncation of the protein chain (CARD1 missing) and subsequent exposure of areas otherwise buried in full-length RIG-I. Hydrophilic areas shown in blue, hydrophobic areas in green. (F) Overall surface charge is similar in the WT (left) and S<sub>183</sub>I (right) structure but individual charged residues are positioned differently. Negative charge shown in red, positive charge in blue. doi:10.1371/journal.pone.0007582.g005

signaling through an increase of RIG-I homocomplexes and RIG-I/MAVS heterocomplexes, it might be speculated that in a heterozygous host, the mutant protein would interfere with the function of the normal protein being produced from the WT allele. To test this hypothesis, we titrated WT RIG-I with increasing amounts of S<sub>183</sub>I RIG-I in mock treated-HEK 293T and in HEK 293T cells activated by the viral mimetic poly(I:C) or infected by Sendai virus (Fig. 6, panels A–C). As a single example, IFN- $\beta$

response was reduced by ~50% in cells co-transfected with an equimolar concentration of WT RIG-I and S<sub>183</sub>I RIG-I expressing vectors and further activated by these stimuli (n = 3,  $p < 0.0001$ ). We also observed that this S<sub>183</sub>I 2CARD mutant reduced IFN- $\beta$  activity of WT 2CARD by ~50% when transfected at a 1:1 ratio and up to 70% at a fourfold excess of transfected plasmid DNA (n = 3,  $p < 0.0001$ , Fig. 6D). Interestingly, the negative impact of S<sub>183</sub>I SNP was less potent when considering

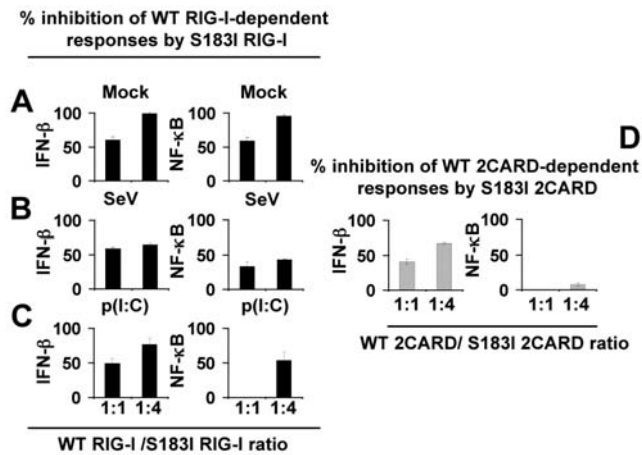


**Figure 6. Down-regulatory effect of S<sub>183</sub>I RIG-I SNP.** (A–C) S<sub>183</sub>I exerts a down-modulatory effect on full-length WT RIG-I-mediated responses as revealed by IFN-β and NF-κB-dependent reporter assays with HEK 293T cells transfected at different ratio with WT RIG-I and/or S<sub>183</sub>I RIG-I vectors. An empty vector was used to maintain the total plasmid quantity constant. Data represent the mean ± SD of percentage of inhibition by S<sub>183</sub>I RIG-I of WT RIG-I-dependent constitutive responses (A, “mock”), or after Sendai virus infection (B), or after challenge by poly(I:C) (p(I:C); C) of triplicate samples. (d) S<sub>183</sub>I exerts a down-regulatory effect on WT 2CARD-induced antiviral, but not on pro-inflammatory, responses. HEK 293T cells were transfected as in (A–C) except that expression of full-length WT or S<sub>183</sub>I RIG-I was replaced by the corresponding 2CARD modules. Data represent the mean ± SD of percentage of inhibition by S<sub>183</sub>I 2CARD of WT 2CARD-dependent constitutive responses measured in triplicate samples. (A–D) are representative of three independent experiments. doi:10.1371/journal.pone.0007582.g006

RIG-I-mediated NF-κB activity triggered by poly(I:C) or tandem 2CARD or Sendai virus, consistently with the primary role of RIG-I in type I-IFN-inducing antiviral signaling pathways [2,3,4,27].

## Discussion

The efforts conducted by international consortiums – such as the HapMap Project and Perlegen – to identify and characterize the levels of polymorphic variation in humans has yielded an ever-growing list of SNPs [28]. These include variation located in genes involved in innate immunity, which may account for individual differences in the response to pathogens. For instance, mutations in TLR2, TLR4, TLR5 and IRAK4 have all been associated with increased risk to develop infectious diseases [13,29,30]. In regard to genes encoding CARD-containing proteins, mutations in the peptidoglycan receptors NOD1 and NOD2 have been associated to several inflammatory disorders, including Crohn’s disease, Blau syndrome and asthma [23]. A non-synonymous SNP in MDA-5 was also reported to show an association with type I diabetes [31]. Remarkably, no human disease has yet been linked to RIG-I. Nonetheless, the defective response of a human hepatoma cell line, found permissive to HCV replication, was due to a single mutation (T<sub>55</sub>I) [9,21,32]. Here, we characterized functional effects of RIG-I SNPs that might help us to understand the basis of individual variations between normal and abnormal innate immune responses to viral pathogens as well as to better appreciate the molecular mechanism by which RIG-I is triggered by non-self RNA.

Among the eight RIG-I SNPs reported in NCBI SNP database, we characterized two distinct functional SNPs which strongly alter

RIG-I-mediated signaling. First, we identified P<sub>229</sub>fS as a SNP which results in a truncated constitutively active RIG-I. This finding is particularly important as it suggests that individuals carrying such mutation may constitutively produce exaggerated amounts of antiviral and pro-inflammatory mediators. Conversely, in agreement with a very recent study from T. Fujita’s laboratory [20], we characterized the loss-of-function S<sub>183</sub>I SNP. Interestingly, this natural mutation allowed us to further demonstrate the importance of S<sub>183</sub> in the transient complex formation that is required for proper RIG-I signaling. Thus, our findings strongly support the hypothesis that regulation of RIG-I/RIG-I and RIG-I/MAVS association/dissociation constitutes a major checkpoint of this antiviral signaling pathway.

CARDs-containing proteins are members of a large group of the ‘death domain superfamily’, which also include the DD (death domain) subfamily and the DED (death effector domain) subfamily. All these domains have a six-helical bundle (H1–H6) structural fold and mediate homotypic interactions within each domain subfamily [22,33,34]. At the amino acid level, the CARD#2 domain of RIG-I differs from other CARDs (see alignment in Fig. S1), whose molecular structures have been previously determined (e.g. MAVS, Apaf-1, RAIDD, Nod1 [22]). We predicted the CARD#2 three-dimensional structure by using comparative/homology modeling in an approach similar to that taken by Potter *et al.* (where MDA-5 and RIG-I CARD#1 were modeled on a experimentally determined MAVS CARD crystal structure) [34]. We were thus able to visualize the structural implications of the S<sub>183</sub>I SNP. In our model, serine 183 maps to helix H6 (*cf.* Ref. [34]). In molecular dynamics studies, which allowed to assess protein flexibility, H6 with S<sub>183</sub> appeared quite flexible and moved perpendicular to the remaining helices in contrast to H6 with I<sub>183</sub> which seemed more rigid. More pertinent, our findings suggest that the replacement of a hydrophilic serine by a hydrophobic isoleucine may alter the flexibility as well as the surface architecture of the CARD#2 domain, in particular the exposure of hydrophobic areas. These changes may enhance and/or stabilize hydrophobic interactions in H6, critical for CARD-CARD interactions between RIG-I *per se* as well as with MAVS. This hypothesis is consistent with studies that have established that hydrophobic residues put constraints on the relative orientations of protein helices [35]; this process being critical for CARD-CARD complex structures [22,34,36]. While additional structural studies outside the scope of this work will be necessary to fully uncover the structural impact of the S183I mutation, our *in silico* analysis points to a potential impact on the basis of helical packing in the RIG-I CARD#2 domain.

Collectively, on the basis of the data presented here, we consider that serine 183 residue plays a central role in the molecular ordering that leads to RIG-I-mediated NF-κB and IRF-3 activation pathways. Nevertheless, one can wonder how S<sub>183</sub>I SNP inhibits RIG-I-induced signaling pathways despite its enhancing effect on RIG-I complexes formation. Based on our biochemical assays and structural modeling showing that this mutation does affect hydrophobicity and flexibility of the CARD#2 domain of RIG-I but does not influence its ligand binding activity, we hypothesize that S<sub>183</sub>I rather induces an abortive conformation of RIG-I, rendering it incapable of downstream signaling. Concerning the inhibitory effect of S<sub>183</sub>I on RIG-I/MAVS-dependent signal transduction, a recent study clearly supports the concept that MAVS association with RIG-I is not *per se* sufficient for inducing immune gene expression [37]. Thus, a splicing form of MAVS called MAVS 1a, which shares little sequence similarity with WT MAVS but still contains CARD domain as well as a TRAF-binding motif, can interact strongly with RIG-I but cannot trigger cell signaling. Therefore, like S<sub>183</sub>I, expression of MAVS 1a interferes with the formation of

productive RIG-I/MAVS signaling complexes, which likely contributes to its inhibitory outcome.

Elucidating the functional role of RIG-I SNPs may enhance our understanding of the pathogenesis of viral infections, to ultimately decrease morbidity and mortality through improved risk assessment and early administration of prophylactic therapies [13,29]. Clinical studies assessing S<sub>183I</sub> SNP frequency in control healthy individuals and patients infected by viruses will certainly clarify the contribution of RIG-I variation to the pathogenesis of viral diseases. Likewise, investigating the clinical relevance of the potent immunostimulatory P<sub>229fs</sub> SNP may be particularly interesting in patients with autoimmune diseases where cytokines play a pivotal pathogenic role. Among them, evidence linking IFN- $\alpha/\beta$  with the pathogenesis of lupus and insulin-dependent diabetes mellitus in humans are the most convincing [38]. Meanwhile, our study demonstrates that serine 183 is a pivotal residue involved in communication between CARD modules of RIG-I themselves as well as with MAVS and emphasizes the complexity of molecular events that governs RIG-I-induced antiviral signaling.

## Materials and Methods

### Viruses and reagents

Influenza A/Scotland/20/74 (H3N2) virus was prepared as previously described [39]. Sendai virus (Cantell strain, ATCC VR-907 Parainfluenza 1) was a kind gift of E. Meurs (Institut Pasteur, Paris, France). The viral dsRNA mimetic polyinosinic: polycytidylic acid (poly(I:C)) and phorbol 12-myristate 13-acetate, (PMA) were from Sigma. Human recombinant TNF $\alpha$  was purchased from Peprotech.

### Phylogenetic analysis of RIG-I SNPs

RIG-I SNPs were as described in NCBF's SNP database (*cf.* [http://www.ncbi.nlm.nih.gov/SNP/snp\\_ref.cgi?locusId=23586](http://www.ncbi.nlm.nih.gov/SNP/snp_ref.cgi?locusId=23586)). RIG-I sequences from human to platypus were aligned using EMBL ClustalW software and manually arranged.

### Plasmids construction and site-directed mutagenesis

The pEFBOS(+)-Flag-RIG-I (amino acids 2–925) or 2CARD (amino acids 2–229) vectors were previously described [17] and pcDNA3-Flag-MAVS and pCI-V5-WT 2CARD plasmids were a kind gift of Dr. Z. Chen and Dr. E. Meurs, respectively. SNPs containing plasmids were made using the QuickChange II XL Site-Directed Mutagenesis kit (Stratagene). Sequences of oligonucleotides used for mutagenesis are indicated in Table S1. An *in vitro* recombination-based cloning (Gateway system; Invitrogen) was used to generate biotin-tagged WT or S<sub>183I</sub> RIG-I, as previously described [40]. Briefly, biotin-tagged RIG-I (WT or S<sub>183I</sub>) expression vectors were generated by PCR using pEFBOS(+)-Flag RIG-I as a template and the following forward (5'-ggggacaactttgtacaaaaaagttggcatgACCACCGAGCAGCGACGCA-3') and reverse primers (5'-ggggacaactttgtacaagaagttggttaTTTGGACATTTCTGCTGGATCAAATGG-3'), as well as the Gateway technology for a final cloning in pcDNA6/BioEase-DEST plasmid (Invitrogen), according to manufacturer's instructions.

All constructs were entirely sequenced to confirm that no unintended mutations were generated during PCR reaction.

### Cell culture, transfection, ELISA and luciferase assays

Detailed protocols were described before [39]. Data are expressed as the mean ( $\times 10^{-3}$ ) of relative luciferase units (RLU) normalized with  $\beta$ -galactosidase activity minus basal activity measured in empty vector-transfected cells.

### Immunoblot and protein-protein interactions analysis

EK 293T cells were transiently co-transfected with 1  $\mu$ g of Flag-tagged MAVS or V5-tagged 2CARD vectors (for tandem 2CARD/MAVS interaction analysis) or 3  $\mu$ g of Flag-tagged 2CARD and biotin-conjugated RIG-I vectors (for tandem 2CARD/RIG-I interaction). After cell disruption and a pre-clearing step, pull-down of biotin-tagged RIG-I was performed using streptavidin sepharose beads (GE Healthcare). For co-immunoprecipitation assay, cell lysates were incubated with a monoclonal anti-Flag M2 antibody, followed by the addition of protein G sepharose beads. More detailed protocols can be provided upon request. After centrifugation and protein denaturation, samples were analyzed by immunoblot as described in reference [39].

### dsRNA binding assay

Assay of dsRNA binding activity of RIG-I (WT or S<sub>183I</sub>) was previously described [41]. Briefly, HEK 293T cells were seeded in 100 mm tissue culture dishes and transiently transfected with 8  $\mu$ g of control plasmid or vector encoding Flag-tagged RIG-I (WT or S<sub>183I</sub>). 48 h post-transfection, cells were disrupted in 1.5 ml of RIPA lysis buffer and 400  $\mu$ g of cell lysates were incubated with poly(I:C)- or control poly(C)-coated agarose beads (Sigma) in RIPA lysis buffer supplemented with proteases inhibitors cocktail and 50 U/ml of RNase inhibitor (Promega) for 1 h at 4°C. Agarose beads were then collected by centrifugation and washed three times with lysis buffer before resuspension in 30  $\mu$ l sample denaturing buffer.

### Flow cytometry and fluorescence microscopy analysis.

To evaluate RIG-I (WT or SNP) protein expression levels and subcellular localization, BEAS-2B and HEK 293T cells were transfected and processed as previously described [42], using the following antibodies: anti-Flag antibody (2  $\mu$ g/ml) and Alexa<sup>488</sup>-conjugated secondary antibody (4  $\mu$ g/ml, A11001, Molecular probes).

### Computational modeling and structural analysis of RIG-I CARD#2

Homology modeling and molecular dynamics of the human RIG-I CARD#2 domain were carried out as previously described by Kubarenko *et al.* [24] based on several CARD domain structures: 1cww [43], 2vgq [34], 3crd [44], 1dgn [45] and 2b1w [46]. The sequence identity for 2vgq and RIG-I CARD domains is between 21–26.8% (depending on the alignment algorithm used). The method of comparative/homology modeling was therefore applied [47]. Structure analysis was carried using the following software (referenced in [24]) SwissPBD Viewer and PyMol ([www.pymol.org](http://www.pymol.org)) for visualization; HotPatch [48] for hydrophobicity and PDB2PQR [49], PropKa [50] and APBS [51] for charged surface calculation. Further details are available on request.

### Statistical analysis

Statistical differences were tested using a one-way ANOVA followed by a Fisher test, with a threshold of  $p < 0.05$ .

### Supporting Information

**Table S1** Plasmids containing SNPs were made by site-directed mutagenesis using the QuickChange II XL Site-Directed Mutagenesis kit (Stratagene), 125 ng of specific forward and reverse primers and 25 ng of RIG-I WT vector as a template in 50  $\mu$ l reaction volume. After an initial denaturation step at 95°C for 1 min, mutagenesis was performed by 18 cycles of amplification (1 min at 95°C, 50 s at 60°C and 9 min 30 s at 68°C), followed by

a final elongation step at 68°C for 7 min. After PCR, template digestion by DpnI restriction enzyme and transformation of bacteria were performed according to manufacturer's instructions. Found at: doi:10.1371/journal.pone.0007582.s001 (0.03 MB DOC)

**Figure S1** Alignment of amino acid sequence of CARD#2 domain of RIG-I with other CARD structures. Alignment of CARD domain sequences from different CARD proteins which were used for RIG-I CARD#2 modeling. Helix 1 colored in red, helix 2 in orange, helix 3 in yellow, helix 4 in green, helix 5 in blue and helix 6 in brown. For Apafl, MAVS, RAIDD, ICEBERG and NOD1 CARDS, helix boundaries were determined directly from the respective PDB files 1cww, 2vgg, 3crd, 1dgn and 2b1w, based on a 3D alignment of these structures. Found at: doi:10.1371/journal.pone.0007582.s002 (0.91 MB DOC)

**Figure S2** Intermediate frames of WT and S183I CARD#2 structures during molecular dynamic simulation. Eleven frames from the molecular dynamics simulation of RIG-I CARD#2 WT (A) or S183I mutant (B), showing one frame per picosecond. First frame (0 ps) corresponds to the initial raw model conformation. Helices from 1 to 6 are rainbow-colored, helix 6 which harbors S183 is colored red. Found at: doi:10.1371/journal.pone.0007582.s003 (4.28 MB DOC)

## References

- Chi H, Flavell RA (2008) Innate recognition of non-self nucleic acids. *Genome Biol* 9: 211.
- Moore CB, Ting JP (2008) Regulation of mitochondrial antiviral signaling pathways. *Immunity* 28: 735–739.
- Takeuchi O, Akira S (2008) MDA5/RIG-I and virus recognition. *Curr Opin Immunol* 20: 17–22.
- Yoneyama M, Fujita T (2008) Structural Mechanism of RNA Recognition by the RIG-I-like Receptors. *Immunity* 29: 178–181.
- Schlee M, Hartmann E, Coch C, Wimmenauer V, Janke M, et al. (2009) Approaching the RNA ligand for RIG-I? *Immunol Rev* 227: 66–74.
- Cheng G, Zhong J, Chisari FV (2006) Inhibition of dsRNA-induced signaling in hepatitis C virus-infected cells by NS3 protease-dependent and -independent mechanisms. *Proc Natl Acad Sci U S A* 103: 8499–8504.
- Saito T, Hirai R, Loo YM, Owen D, Johnson CL, et al. (2007) Regulation of innate antiviral defenses through a shared repressor domain in RIG-I and LGP2. *Proc Natl Acad Sci U S A* 104: 582–587.
- Kato H, Takeuchi O, Sato S, Yoneyama M, Yamamoto M, et al. (2006) Differential roles of MDA5 and RIG-I helicases in the recognition of RNA viruses. *Nature* 441: 101–105.
- Sumpter R, Jr., Loo YM, Foy E, Li K, Yoneyama M, et al. (2005) Regulating intracellular antiviral defense and permissiveness to hepatitis C virus RNA replication through a cellular RNA helicase, RIG-I. *J Virol* 79: 2689–2699.
- Binder M, Kochs G, Bartenschlager R, Lohmann V (2007) Hepatitis C virus escape from the interferon regulatory factor 3 pathway by a passive and active evasion strategy. *Hepatology* 46: 1365–1374.
- Lloyd AR, Jagger E, Post JJ, Crooks LA, Rawlinson WD, et al. (2007) Host and viral factors in the immunopathogenesis of primary hepatitis C virus infection. *Immunol Cell Biol* 85: 24–32.
- Reiche EM, Bonametti AM, Voltarelli JC, Morimoto HK, Watanabe MA (2007) Genetic polymorphisms in the chemokine and chemokine receptors: impact on clinical course and therapy of the human immunodeficiency virus type 1 infection (HIV-1). *Curr Med Chem* 14: 1325–1334.
- Misch EA, Hawn TR (2008) Toll-like receptor polymorphisms and susceptibility to human disease. *Clin Sci (Lond)* 114: 347–360.
- Ramensky V, Bork P, Sunyaev S (2002) Human non-synonymous SNPs: server and survey. *Nucleic Acids Res* 30: 3894–3900.
- Le Goffic R, Pothlichet J, Vitour D, Fujita T, Meurs E, et al. (2007) Cutting Edge: Influenza A virus activates TLR3-dependent inflammatory and RIG-I-dependent antiviral responses in human lung epithelial cells. *J Immunol* 178: 3368–3372.
- Yoneyama M, Kikuchi M, Matsumoto K, Imaizumi T, Miyagishi M, et al. (2005) Shared and unique functions of the DExD/H-box helicases RIG-I, MDA5, and LGP2 in antiviral innate immunity. *J Immunol* 175: 2851–2858.
- Yoneyama M, Kikuchi M, Natsukawa T, Shinobu N, Imaizumi T, et al. (2004) The RNA helicase RIG-I has an essential function in double-stranded RNA-induced innate antiviral responses. *Nat Immunol* 5: 730–737.
- Cheng G, Zhong J, Chung J, Chisari FV (2007) Double-stranded DNA and double-stranded RNA induce a common antiviral signaling pathway in human cells. *Proc Natl Acad Sci U S A* 104: 9035–9040.
- Hausmann S, Marq JB, Tapparel C, Kolakofsky D, Garcin D (2008) RIG-I and dsRNA-induced IFN $\beta$  activation. *PLoS One* 3: e3965.
- Shigemoto T, Kagayama M, Hirai R, Zheng J, Yoneyama M, et al. (2009) Identification of loss of function mutations in human genes encoding RIG-I and mda5: Implications for resistance to type I diabetes. *J Biol Chem* 284: 13348–13354.
- Gack MU, Shin YC, Joo CH, Urano T, Liang C, et al. (2007) TRIM25 RING-finger E3 ubiquitin ligase is essential for RIG-I-mediated antiviral activity. *Nature* 446: 916–920.
- Park HH, Lo YC, Lin SC, Wang L, Yang JK, et al. (2007) The death domain superfamily in intracellular signaling of apoptosis and inflammation. *Annu Rev Immunol* 25: 561–586.
- Werts C, Girardin SE, Philpott DJ (2006) TIR, CARD and PYRIN: three domains for an antimicrobial triad. *Cell Death Differ* 13: 798–815.
- Kubarenko A, Frank M, Weber AN (2007) Structure-function relationships of Toll-like receptor domains through homology modelling and molecular dynamics. *Biochem Soc Trans* 35: 1515–1518.
- Gregersen N (2006) Protein misfolding disorders: pathogenesis and intervention. *J Inher Metab Dis* 29: 456–470.
- Sanders CR, Ismail-Beigi F, McEnery MW (2001) Mutations of peripheral myelin protein 22 result in defective trafficking through mechanisms which may be common to diseases involving tetraspan membrane proteins. *Biochemistry* 40: 9453–9459.
- Schroder M, Bowie AG (2007) An arms race: innate antiviral responses and counteracting viral strategies. *Biochem Soc Trans* 35: 1512–1514.
- Hinds DA, Stuve LL, Nilsen GB, Halperin E, Eskin E, et al. (2005) Whole-genome patterns of common DNA variation in three human populations. *Science* 307: 1072–1079.
- Tebbutt SJ, James A, Pare PD (2007) Single-nucleotide polymorphisms and lung disease: clinical implications. *Chest* 131: 1216–1223.
- Picard C, von Bernuth H, Ku CL, Yang K, Puel A, et al. (2007) Inherited human IRAK-4 deficiency: an update. *Immunol Res* 38: 347–352.
- Smyth DJ, Cooper JD, Bailey R, Field S, Burren O, et al. (2006) A genome-wide association study of nonsynonymous SNPs identifies a type 1 diabetes locus in the interferon-induced helicase (IFIH1) region. *Nat Genet* 38: 617–619.
- Gack MU, Kirchhofer A, Shin YC, Inn KS, Liang C, et al. (2008) Roles of RIG-I N-terminal tandem CARD and splice variant in TRIM25-mediated antiviral signal transduction. *Proc Natl Acad Sci U S A* 105: 16743–16748.
- Palsson-McDermott EM, O'Neill LA (2007) Building an immune system from nine domains. *Biochem Soc Trans* 35: 1437–1444.
- Potter JA, Randall RE, Taylor GL (2008) Crystal structure of human IPS-1/MAVS/VISA/Cardif caspase activation recruitment domain. *BMC Struct Biol* 8: 11.

35. Dyson HJ, Wright PE, Scheraga HA (2006) The role of hydrophobic interactions in initiation and propagation of protein folding. *Proc Natl Acad Sci U S A* 103: 13057–13061.
36. Zhou P, Chou J, Olea RS, Yuan J, Wagner G (1999) Solution structure of Apaf-1 CARD and its interaction with caspase-9 CARD: a structural basis for specific adaptor/caspase interaction. *Proc Natl Acad Sci U S A* 96: 11265–11270.
37. Lad SP, Yang G, Scott DA, Chao TH, Correia Jda S, et al. (2008) Identification of MAVS splicing variants that interfere with RIGI/MAVS pathway signaling. *Mol Immunol* 45: 2277–2287.
38. Theofilopoulos AN, Baccala R, Beutler B, Kono DH (2005) Type I interferons (alpha/beta) in immunity and autoimmunity. *Annu Rev Immunol* 23: 307–336.
39. Pothlichet J, Chignard M, Si-Tahar M (2008) Cutting edge: innate immune response triggered by influenza A virus is negatively regulated by SOCS1 and SOCS3 through a RIG-I/IFNAR1-dependent pathway. *J Immunol* 180: 2034–2038.
40. Caignard G, Guerbois M, Labernardiere JL, Jacob Y, Jones LM, et al. (2007) Measles virus V protein blocks Jak1-mediated phosphorylation of STAT1 to escape IFN-alpha/beta signaling. *Virology* 368: 351–362.
41. Rothenfusser S, Goutagny N, DiPerna G, Gong M, Monks BG, et al. (2005) The RNA helicase Lgp2 inhibits TLR-independent sensing of viral replication by retinoic acid-inducible gene-I. *J Immunol* 175: 5260–5268.
42. Guillot L, Medjane S, Le-Barillec K, Balloy V, Danel C, et al. (2004) Response of human pulmonary epithelial cells to lipopolysaccharide involves Toll-like receptor 4 (TLR4)-dependent signaling pathways: evidence for an intracellular compartmentalization of TLR4. *J Biol Chem* 279: 2712–2718.
43. Day CL, Dupont C, Lackmann M, Vaux DL, Hinds MG (1999) Solution structure and mutagenesis of the caspase recruitment domain (CARD) from Apaf-1. *Cell Death Differ* 6: 1125–1132.
44. Chou JJ, Matsuo H, Duan H, Wagner G (1998) Solution structure of the RAIDD CARD and model for CARD/CARD interaction in caspase-2 and caspase-9 recruitment. *Cell* 94: 171–180.
45. Humke EW, Shriver SK, Starovasnik MA, Fairbrother WJ, Dixit VM (2000) ICEBERG: a novel inhibitor of interleukin-1beta generation. *Cell* 103: 99–111.
46. Manon F, Favier A, Nunez G, Simorre JP, Cusack S (2007) Solution structure of NOD1 CARD and mutational analysis of its interaction with the CARD of downstream kinase RICK. *J Mol Biol* 365: 160–174.
47. Sanchez R, Sali A (2000) Comparative protein structure modeling. Introduction and practical examples with modeller. *Methods Mol Biol* 143: 97–129.
48. Pettit FK, Bare E, Tsai A, Bowie JU (2007) HotPatch: a statistical approach to finding biologically relevant features on protein surfaces. *J Mol Biol* 369: 863–879.
49. Dolinsky TJ, Nielsen JE, McCammon JA, Baker NA (2004) PDB2PQR: an automated pipeline for the setup of Poisson-Boltzmann electrostatics calculations. *Nucleic Acids Res* 32: W665–667.
50. Li H, Robertson AD, Jensen JH (2005) Very fast empirical prediction and rationalization of protein pKa values. *Proteins* 61: 704–721.
51. Baker NA, Sept D, Joseph S, Holst MJ, McCammon JA (2001) Electrostatics of nanosystems: application to microtubules and the ribosome. *Proc Natl Acad Sci U S A* 98: 10037–10041.